University of Nebraska - Lincoln
DigitalCommons@University of Nebraska - Lincoln

Christian Binek Publications | Research Papers in Physics and Astronomy

11-25-2003

Giant metamagnetic moments in a granular $FeCl_2$-Fe heterostructure

Sarbeswar Sahoo
Angewandte Physik, Universität Duisburg-Essen, Duisburg, Germany, sarbeswar@gmail.com

Christian Binek
University of Nebraska-Lincoln, cbinek@unl.edu

Wolfgang Kleemann
Angewandte Physik, Universität Duisburg-Essen, Duisburg, Germany, wolfgang.kleemann@uni-due.de

Follow this and additional works at: http://digitalcommons.unl.edu/physicsbinek

 Part of the Physics Commons

Sahoo, Sarbeswar; Binek, Christian; and Kleemann, Wolfgang, "Giant metamagnetic moments in a granular $FeCl_2$-Fe heterostructure" (2003). *Christian Binek Publications*. 22.
http://digitalcommons.unl.edu/physicsbinek/22

This Article is brought to you for free and open access by the Research Papers in Physics and Astronomy at DigitalCommons@University of Nebraska - Lincoln. It has been accepted for inclusion in Christian Binek Publications by an authorized administrator of DigitalCommons@University of Nebraska - Lincoln.

Giant metamagnetic moments in a granular $FeCl_2$-Fe heterostructure

Sarbeswar Sahoo, Christian Binek, and Wolfgang Kleemann
Angewandte Physik, Universität Duisburg-Essen, D-47048 Duisburg, Germany
(Received 17 June 2003; published 25 November 2003)

Giant moments are observed at low temperatures in a granular $FeCl_2$-Fe heterostructure owing to a local metamagnetic transformation of the antiferromagnetic (AF) $FeCl_2$ matrix due to dipolar interactions. A model of metamagnetically (MM) "dressed" single-domain Fe particles is suggested to explain the observations. These include polydispersive ac susceptibility induced by AF-MM domain configurations and weak exchange bias due to non-spin-flipped AF crystallites.

DOI: 10.1103/PhysRevB.68.174431 PACS number(s): 75.70.−i, 75.60.Nt, 75.50.Ee

The physics of ferromagnetic (FM) nanoparticles which are embedded in an insulating matrix is one of the major topics of recent research activities in magnetism because of their interesting magnetic[1–3] as well as electronic transport properties.[4] Up to now, the nanoparticles have been embedded in insulating diamagnetic matrices such as Al_2O_3, SiO_2, HfO_2 or frozen carrier liquids such as kerosene. Various magnetic states such as superparamagnetic blocking,[1] collective superspin-glass freezing,[2] and superferromagnetism[3] have been revealed at different packing densities of the nanoparticles. In these systems, the interaction of the nanoparticles with the host matrix has been neglected. In contrast, the particle-matrix interaction becomes significant when the diamagnetic matrix is replaced, e.g., by an antiferromagnetic (AF) one. Indeed, the first study of fine Co particles embedded in their native oxide led to the discovery of unidirectional anisotropy which gives rise to an exchange bias (EB) of the hysteresis loop due to exchange coupling at the FM-AF interface.[5] The phenomenon was later on observed in many other FM-AF fine particle systems and in continuous films consisting of sandwiched AF and FM layers.[6] Recent experiments have confirmed that the alignment of FM spins in these exchange-coupled systems is determined by the spin directions in the underlaying AF layer giving rise to exchange bias.[7]

On the other hand, also the retroactivity of the FM nanoparticles onto the AF matrix may be of interest. Most spectacular effects are expected if the AF intramatrix exchange is weak compared to its interaction with the embedded FM nanoparticles. It will be due to the combined effects of exchange coupling at the particle-matrix interface and their dipolar stray fields. Here we report on the experimental investigation of a granular $FeCl_2$-Fe heterostructure which clearly evidences formation of giant metamagnetic (MM) moments containing Fe granules as nucleation cores. Temperature- and frequency-dependent ac-susceptibility measurements hint at the presence of a mixed AF-MM state with polydispersive domain wall susceptibility. To the best of our knowledge, it is the first time that such a mechanism is observed in an AF-FM granular system.

The sample investigated in this study was prepared by coevaporation of $FeCl_2$ and Fe in an ultrahigh vacuum (1×10^{-10} mbars) molecular-beam epitaxy chamber on a sapphire $(11\bar{2}0)$ substrate. After rinsing in acetone the sapphire substrate was preheated to 300 °C for 1 h in order to degas it and then cooled to and maintained at liquid N_2 temperature during the evaporation processes. As a result $FeCl_2$ becomes amorphous, which warrants tight embedding of the Fe particles during the growth. Upon room temperature annealing $FeCl_2$ eventually recrystallizes and recovers its original bulk properties.[8] The $FeCl_2$:29 vol.% Fe layer with a thickness of 500 nm was sandwiched between two 200-nm $FeCl_2$ layers and capped by a 50-nm gold layer. A room-temperature wide-angle x-ray diffraction pattern of the sample showed polycrystallinity of $FeCl_2$ with grain sizes of about 80 nm and nanocrystallinity of Fe with particle diameters $D\approx10$ nm immediately after evaporation. Details of the microstructural characterization will be published elsewhere.[9]

Dc magnetization and ac susceptibility measurements were performed by use of a commercial superconducting quantum interference device magnetometer (MPMS-5S, Quantum Design). For zero-field-cooling field-heating (ZFC-FH) measurements, the sample was cooled from high temperature (290 or 360 K) in zero field to 5 K where a field step is applied and magnetization is recorded upon heating. The subsequent cooling in the same field is called FC, while thermoremanent magnetization (TRM) is recorded during the following reheating after switching off the field.

Figure 1 shows the ZFC-FH, FC, and TRM magnetizations ($m^{\mathrm{ZFC\text{-}FH}}$, m^{FC}, and m^{TRM}, respectively) vs temperature involving an external magnetic field of $\mu_0H=10$ mT. It follows a demagnetization procedure at $T=290$ K, where the sample is saturated at $\mu_0H=2$ T and the field is reduced to zero in alternated cycles (saturation-reverse-zero), thus producing random orientations of Fe moments. The corresponding blocking of Fe granules, characterized by an irreversibility between $m^{\mathrm{ZFC\text{-}FH}}$ and m^{FC} occurs at $T_b\approx320$ K as shown in the upper inset to Fig. 1. Using the Arrhenius-Néel-Brown blocking ansatz,[10,11] $\tau=\tau_0\exp(KV/k_BT_b)$, and associating an observation time of 100 s to our measurement, it was found that this value of blocking temperature corresponds to Fe particles of diameter $D_{\mathrm{Fe}}=16$ nm. Here we have used $\tau_0=10^{-9}$ s and the value of the anisotropy constant $K=5\times10^4$ Jm^{-3} for bulk Fe. Obviously, the result hints at coarse graining of the Fe granules in the early stage of our experiments which finally end up at $D_{\mathrm{Fe}}=16$ nm. It is further noticed that in contrast to the usual blocking behavior of Stoner-Wohlfarth particles[12] the here-observed irreversibility

 ©2003 The American Physical Society

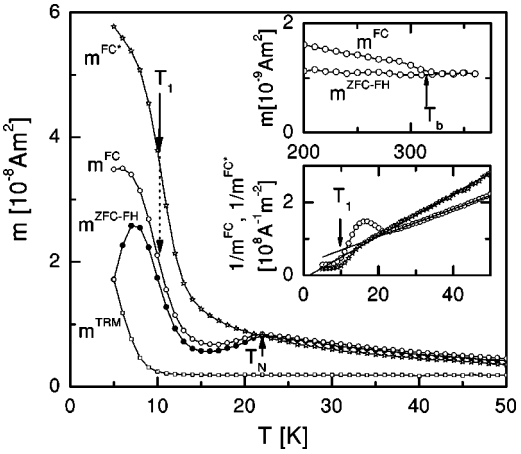

FIG. 1. (a) $m^{\mathrm{ZFC\text{-}FH}}$, m^{FC}, $m^{\mathrm{FC}*}$, and m^{TRM} vs temperature T involving an external magnetic field of $\mu_0 H = 10$ mT. The arrows indicate the corresponding Néel temperature $T_{\mathrm{N}} \approx 22$ K and point of inflexion, $T_1 \approx 10$ K, of m^{FC} and of $m^{\mathrm{FC}}*$. The upper inset shows the irreversibility between $m^{\mathrm{ZFC\text{-}FH}}$ and m^{FC} taking place at $T_{\mathrm{b}} \approx 320$ K. The lower inset shows $1/m^{\mathrm{FC}}$ and $1/m^{\mathrm{FC}}*$ vs T and Curie-Weiss-type fits (straight lines).

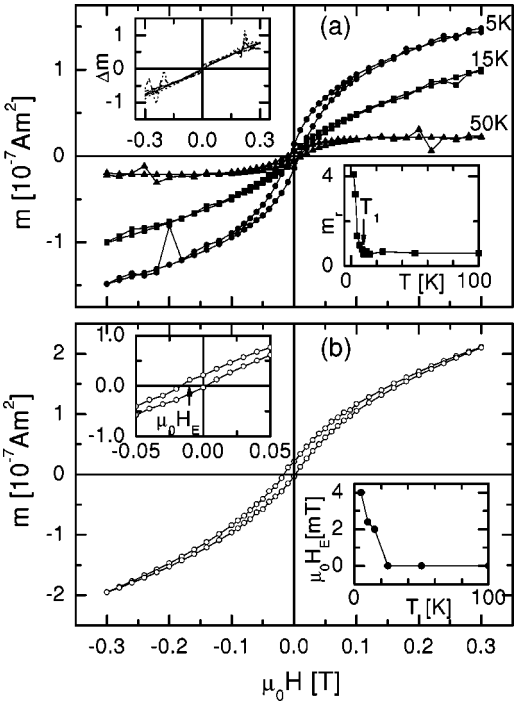

FIG. 2. (a) $m(\mu_0 H)$ loops at some selected temperatures. The lower inset shows the remanent magnetization vs T and T_1 by an arrow. The upper inset shows Δm vs applied magnetic field at the same temperatures as $m(\mu_0 H)$ loops shown in the main panel. (b) $m(\mu_0 H)$ loop at $T = 5$ K after cooling in a field of $\mu_0 H = 0.1$ T. The upper inset shows a magnified portion of the loop with the exchange-bias field $\mu_0 H_{\mathrm{E}}$ indicated by an arrow. The lower inset shows $\mu_0 H_{\mathrm{E}}$ vs T.

exhibits the superimposed features of blocked Fe particles and a Curie-Weiss (CW)-type increase of the magnetization of the AF $FeCl_2$ matrix upon cooling. We point out that both $m^{\mathrm{ZFC\text{-}FH}}$ and m^{FC} of the upper inset figure show identical features below T_{b} as in the demagnetized case (Fig. 1, main panel) except for a constant upward shift of the m^{FC} part owing to the irreversibility at T_{b}.

As seen in Fig. 1, m^{FC} bears much of the behavior of the pure AF $FeCl_2$ matrix, viz., a peak at the ordering temperature $T_{\mathrm{N}} \approx 22$ K and a CW-type decrease at $T > T_{\mathrm{N}}$. However, large enhancement arises in the AF regime below $T \approx 15$ K. An accelerated increase of m^{FC} below the point of inflexion at $T_1 \approx 10$ K and saturation tendencies as $T \to 0$ (Fig. 1, lower inset) seem to reflect metamagnetism of the $FeCl_2$ environment beyond the spin-flip transition,[13] which is induced by the field-aligned Fe granules. Comparison of $m^{\mathrm{FC}}(T = 5\ \mathrm{K}) \approx 3.5 \times 10^{-8}\ \mathrm{A\,m^2}$ with the saturation moment of bare Fe granules $m_{\mathrm{s}} \approx 2 \times 10^{-8}\ \mathrm{A\,m^2}$ in the magnetization hysteresis loop at $T = 50\ \mathrm{K} > T_{\mathrm{N}}$ [see Fig. 2(a)] shows that the total moment of Fe granules is by a factor of about 2 smaller than the anomaly induced by a freezing field as small as $\mu_0 H = 10$ mT. We therefore suggest the enhancement of the FM polarization to be due to the AF matrix within a model of ''dressed'' Fe granules. They are considered as magnetic dipoles, whose stray field in the AF environment maximizes in the polar direction and is given by[14] $\mu_0 H = 2\mu_0 m / 4\pi r'^3$, where r' is the distance between the granule center and the point, where the dipolar field is calculated, and m is the magnetic moment of the dipole as indicated in Fig. 3(a). Assuming spherical shape of the granules with radius r and homogeneous magnetization M_{s}, the above formula holds exactly for $r' \geqslant r$ and can be written as $\mu_0 H = (2/3)\mu_0 M_{\mathrm{s}} / (r'/r)^3$.[15] Taking the saturation magnetization value of bulk Fe (Ref. 16) $M_{\mathrm{s}} = 2.15$ T, the field at the poles is 1.44 T. This value exceeds the spin-flip field which is $\mu_0 H_{\mathrm{SF}} = 1.06$ T at $T = 4.2$ K.[13] At the poles the stray field is nearly parallel with respect to the magnetization of a given Fe granule. Hence, taking into account the preferential alignment of the granule magnetization along the freezing field, one expects a net FM polarization of that part of the $FeCl_2$ matrix whose [111] direction comes close to that of the aligning field. A considerable fraction of the $FeCl_2$ may have unfavorable orientation which does not contribute to the enhancement effect. However, it is obvious that the favorable fraction suffices to produce the observed giant moments. Figure 3(a) schematically depicts the distribution of MM regions emerging from the magnetic poles of the nanoparticle by assuming perfect [111] orientation of the $FeCl_2$ matrix. Since the exchange interaction is short ranged it will merely affect the interfacial spins while the spins at larger distances undergo a local spin-flip transition due to the long-ranged dipolar fields.

Interestingly, the observed m^{TRM} in Fig. 1 obeys the well-known rule of Stoner and Wohlfarth,[12] which predicts $m^{\mathrm{TRM}}(T = 5\ \mathrm{K}) = m_s/2$, where m_{s} is the saturation value m^{FC} $(T = 5\ \mathrm{K})$. Obviously also the dressed moments reorient onto the field-selected hemisphere in the same way as the bare SW particles are used to do. It is further observed that m^{TRM} decays rapidly to an almost constant value at $T > T_1$. It corresponds to the remanence of bare Fe nanoparticles as shown in Fig. 2(a) (lower inset). Clearly the lacking alignment of the Fe moments causes a destabilization of the metamagnetic coating at slightly enhanced temperatures. This is

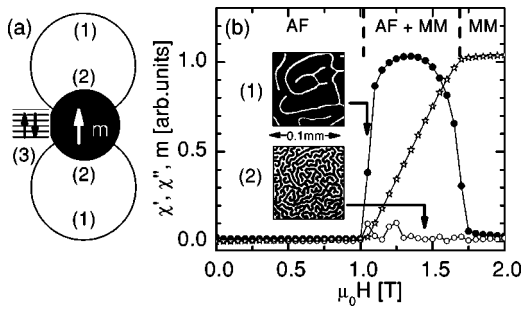

FIG. 3. (a) Schematic geometry of a Fe nanoparticle (black) dressed by MM polar caps (white), which are supposed to contain the domain structures (1) and (2) at the indicated places. Exchange bias producing crystallites (3) are expected along the equatorial belt. (b) Field dependence of the parallel susceptibility components ($f=20$ Hz, $T=10$ K) and of the magnetization of $FeCl_2$, χ', χ'' and m vs $\mu_0 H$ (solid and open circles and asterisks, respectively), revealing large domain-wall contributions in the mixed AF+MM phase, which is due to demagnetization effects. Typical domain structures obtained by Faraday contrast microscopy (black = AF, white = MM) are shown for $\mu_0 H=1.1$ (1) and 1.4 T (2) (Ref. 17).

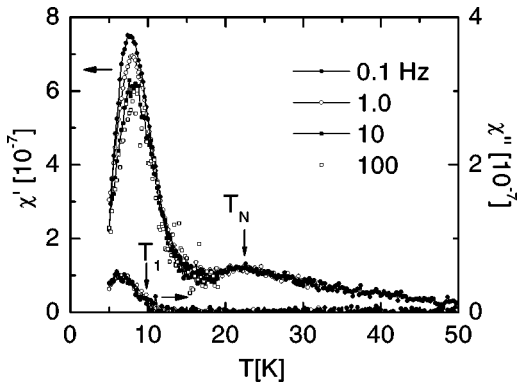

FIG. 4. Temperature variation of ZFC ac susceptibility at $\mu_0 H_{ac}=0.4$ mT and $0.1\leqslant f\leqslant 100$ Hz measured in zero dc bias field.

primarily due to the strong dependence of the spin-flip transition on the field orientation. The zero-field cooled magnetization $m^{\mathrm{ZFC\text{-}FH}}$ vs T achieves no more than 50–80 % of the value of m^{FC} vs T (Fig. 1). The largest difference occurs at low temperatures, $T\approx 5$ K, as a consequence of the poor in-field alignment of the randomly oriented blocked Fe moments. This is partially lifted upon heating where a peak arises at $T\approx 8$ K, while $m^{\mathrm{ZFC\text{-}FH}}$ and m^{FC} perfectly coincide above T_{N}.

The growth of the metamagnetic moments has been verified by measuring the FC magnetization without a demagnetization procedure at $T=290$ K or, equivalently, without crossing the blocking temperature $T_{\mathrm{b}}\approx 320$ K of the Fe particles. This is shown in Fig. 1 by the data designated as $m^{\mathrm{FC}*}$ vs T, which are obtained with the same external field of $\mu_0 H=10$ mT on cooling from $T=290$ K from a premagnetized state. Remarkably, $m^{\mathrm{FC}*}$ shows no anomaly at the AF transition, which is more clearly seen when plotting $1/m^{\mathrm{FC}*}$ vs T (Fig. 1, lower inset). Obviously, the perfectly field-aligned Fe particles having a volume fraction of 29% destroy the long-range AF ordering of the $FeCl_2$ very efficiently due to the constructive superposition of the local stray fields. In particular, the extrapolated positive Curie-Weiss temperature $\theta_C\approx 2$ K seems to indicate ferromagnetic correlations. Indeed, drastically enhanced magnetization values occur below the inflexion point at $T<T_1$. Obviously the blocked field-aligned Fe granules convert a larger AF surrounding into a FM one by virtue of an enhanced dipolar field strength. The observed enhancement by 70% at $T=5$ K hints at a radial increase by 20% when assuming a homogeneous spherical distribution of FM moments. It is worth mentioning that the corresponding $m^{\mathrm{ZFC\text{-}FH}*}$ and $m^{\mathrm{TRM}*}$ data are identical to those of the demagnetized system.

In order to clarify the nature of the low-temperature properties, ac-susceptibility measurements were performed following an identical procedure as described in Fig. 1. An ac amplitude of $\mu_0 H_{ac}=0.4$ mT and frequencies in the range $0.1\leqslant f\leqslant 100$ Hz were employed. In Fig. 4, the temperature variation of the real part of the ac susceptibility, χ', shows two distinct peaks in much the same way as $m^{\mathrm{ZFC\text{-}FH}}$ vs T in Fig. 1. The frequency-independent peak at $T_{\mathrm{N}}\approx 22$ K characterizes the AF feature. The pronounced lower-temperature peak, again, clearly signifies local FM transformation of the AF environment. Its frequency dependence and a concomitant appearance of an imaginary component χ'' below $T_1\approx 10$ K hint at polydispersive processes. They are probably due to AF-MM interfaces, which are expected to occur within the spin-flipped regions of the matrix. It has to be noticed that neither the purely AF nor the purely MM phase has an appreciable susceptibility response at low temperatures. This is shown in Fig. 3(b) for χ' vs $\mu_0 H$ as measured on a $FeCl_2$ crystal plate (thickness 0.4 mm) at $f=20$ Hz and $T=10$ K in a [111]-directed field, $0\leqslant\mu_0 H\leqslant 2$ T. Large signals arise only in the mixed phase region, designated as AF +MM, within $1.05\leqslant\mu_0 H\leqslant 1.75$ T, where $FeCl_2$ develops meandering stripe domains with increasing contents of the MM phase as $\mu_0 H$ increases. Two typical domain structures as imaged by Faraday microscopy[17] at $\mu_0 H=1.1$ (1) and 1.4 T (2) are shown in Fig. 3(b) and supposed to appear far from and close to the nanoparticular poles, respectively, as indicated in Fig. 3(a). Nonvanishing losses χ'' [Fig. 3(b), open circles] are also restricted to the mixed phase, where the magnetization m increases linearly [Fig. 3(b), asterisks].

Figure 2(a) presents the M vs $\mu_0 H$ loops measured at $T=50$, 15, and 5 K, i.e., above and below the Néel temperature, in the field range $-0.3\leqslant\mu_0 H\leqslant 0.3$ T after ZFC from $T=350$ K$>T_{\mathrm{b}}$. At $T=50$ K the finite remanence and coercivity are reminiscent of the hysteretic behavior of blocked Fe granules which are unaffected by the paramagnetic $FeCl_2$ matrix. At $T<T_{\mathrm{N}}$ the magnitude of the magnetization increases by one order of magnitude, although the applied fields are insufficient to cause a spin-flip transition of the $FeCl_2$ matrix ($\mu_0 H_{\mathrm{SF}}=1.06$ T). This underlines the conjectured growth of dressed granules by virtue of the dipolar interaction with the AF matrix. It is remarked that there is a qualitative difference between the loops above and below T_1, where Fe granules become dressed. In the upper inset, we show the difference between the magnetic moment at low temperatures and the scaled reference curve $m(H,T$

$=50$ K), $\Delta m = m(H,T) - \lambda(T) m(H, T=50\ \mathrm{K})$. $\lambda(T)$ is a variable that measures the enhancement of the effective moment of the dressed Fe granule with respect to the bare one. When choosing $\lambda = 1$, 2.2, and 3 at $T = 15$, 10, and 5 K, respectively, a unique linear curve $\Delta m(H)$ is obtained, which does not depend on the temperature [Fig. 2(a), upper inset]. This result suggests that $\Delta m(H)$ originates from the perpendicular susceptibility $\chi_\perp$ of the AF matrix because the parallel susceptibility $\chi_\parallel$ is much smaller than $\chi_\perp$ far below T_N. On the other hand, the increase of λ clearly reinforces the model assumption of dressed Fe granules, which are estimated to grow in size by about 40% when cooling from $T = 15$ K to 5 K. In accordance with the observed increase of λ the temperature variation of the remanent magnetization m_r shown in the lower inset to Fig. 2(a) reveals a steep rise below T_1.

Figure 2(b) shows the M vs $\mu_0 H$ loop at $T = 5$ K after cooling the sample from $T = 350$ K in a field of $\mu_0 H = 0.1$ T. The shift along the field axis by $\mu_0 H_E = -4$ mT (upper inset) seems to be the fingerprint of EB. This is not expected to occur, if all the magnetization experienced during the hysteresis cycle would be due to the metamagnetic reaction of the AF matrix to magnetization reversal of the Fe granules. However, there are regions where interfacial exchange between the FM granule and the AF matrix dominates. The equatorial belt of the nanoparticle is a dipolar low-field region, where adjacent adequately oriented $FeCl_2$ grains may give rise to EB after properly FC to below T_N. Figure 3(a) indicates how EB active $FeCl_2$ layers have to be oriented with respect to a Fe nanoparticle and its magnetization m. Interestingly, apart from $\mu_0 H_E < 0$ also an upward shift of the hysteresis loop is encountered in Fig. 2(b). Obviously a permanent positive moment is retained in the AF, whose surface component $S_{AF} > 0$ is supposed to control the EB during the field cycles.[18–20] Figure 2(b) (lower inset) shows the temperature dependence of the apparent exchange-bias field $\mu_0 H_E$. As expected, it vanishes along with the disappearance of the trapped moment above the Néel temperature of the AF matrix.

In summary, we have demonstrated that a spectacular enhancement of the magnetization of a granular $FeCl_2$-Fe system occurs below the Néel temperature of $FeCl_2$. It is due to the specific composition of our system, consisting of mesoscopic blocked Fe moments in a microcrystalline AF matrix. Among the secondary effects we have observed an ac susceptibility anomaly, which probably reflects the domain structure within the MM phase, and exchange bias, which reflects the exchange coupling of non-spin-flipped parts of the AF matrix to the Fe nanoparticles. In the light of our results it is concluded that particle-matrix interaction plays a vital role in determining the behavior of granular AF-FM systems. As an outlook to future work it is worth mentioning that doping of an AF matrix with FM nanoparticles may also lead to important consequences on the transport properties, viz., exchange-biased asymmetric tunnel magnetoresistance.

This work was supported by the Deutsche Forschungsgemeinschaft within the framework of the Graduate School 277, ''Structure and Dynamics of Heterogeneous Systems.''

[1] J.L. Dormann, D. Fiorani, and E. Tronc, Adv. Chem. Phys. **98**, 283 (1997).

[2] C. Djurberg, P. Svedlindh, P. Nordblad, M.F. Hansen, F. Bodker, and S. Morup, Phys. Rev. Lett. **79**, 5154 (1997); H. Mamiya, I. Nakatani, and T. Furubayashi, *ibid.* **80**, 177 (1998); J.L. Dormann, D. Fiorani, R. Cherkaoui, E. Tronc, F. Lucari, F. D'Orazio, L. Spinu, M. Nogués, H. Kachkachi, and J.P. Jolivet, J. Magn. Magn. Mater. **203**, 23 (1999); S. Sahoo, O. Petracic, Ch. Binek, W. Kleemann, J.B. Sousa, S. Cardoso, and P.P. Freitas, Phys. Rev. B **65**, 134406 (2002); S. Sahoo, O. Petracic, W. Kleemann, P. Nordblad, S. Cardoso, and P.P. Freitas, *ibid.* **67**, 214422 (2003).

[3] X. Chen, O. Sichelschmidt, W. Kleemann, O. Petracic, Ch. Binek, J.B. Sousa, S. Cardoso, and P.P. Freitas, Phys. Rev. Lett. **89**, 137203 (2002).

[4] L.F. Schelp, A. Fert, F. Fettar, P. Holody, S.F. Lee, J.L. Maurice, F. Petroff, and A. Vaurès, Phys. Rev. B **56**, R5747 (1997); S. Sankar, A.E. Berkowitz, and D.J. Smith, Appl. Phys. Lett. **73**, 535 (1998); Phys. Rev. B **62**, 14 273 (2000); C.T. Black, C.B. Murray, R.L. Sandstrom, and S. Sun, Science **290**, 1131 (2000).

[5] W.H. Meiklejohn and C.P. Bean, Phys. Rev. **105**, 904 (1956).

[6] J. Nogués and I.K. Schuller, J. Magn. Magn. Mater. **192**, 203 (1999).

[7] F. Nolting, A. Scholl, J. Stöhr, J.W. Seo, J. Fompeyrine, H. Siegwart, J.-P. Locquet, S. Anders, J. Lüning, E.E. Fullerton, M.F. Toney, M.R. Scheinfein, and H.A. Padmore, Nature (London) **405**, 767 (2000).

[8] W. Kleemann and B. Hendel, J. Magn. Magn. Mater. **31–34**, 581 (1983).

[9] S. Sahoo, Ch. Binek, and W. Kleemann, *Phase Transitions* (in press).

[10] L. Néel, Ann. Geophys. **5**, 99 (1949).

[11] W.F. Brown, Jr., Phys. Rev. **130**, 1677 (1963).

[12] E.C. Stoner and E.P. Wohlfarth, Philos. Trans. R. Soc. London, Ser. A **240**, 599 (1948).

[13] I.S. Jacobs and P.E. Lawrence, Phys. Rev. **164**, 866 (1967).

[14] B.D. Cullity, *Introduction to Magnetic Materials* (Addison-Wesley, Reading, MA, 1972), p. 614.

[15] A. Aharoni, *Introduction to the Theory of Ferromagnetism* (Oxford Univ. Press, Oxford, 2000), p. 112.

[16] S. Chikazumi, *Physics of Ferromagnetism* (Oxford Univ. Press, Oxford, 1999).

[17] J. Kushauer, Ph.D. thesis, Gerhard-Mercator-Universität, Duisburg, 1995.

[18] K. Takano, R.H. Kodama, A.E. Berkowitz, W. Cao, and G. Thomas, Phys. Rev. Lett. **79**, 1130 (1997).

[19] J. Nogués, C. Leighton, and I.K. Schuller, Phys. Rev. B **61**, 1315 (2000).

[20] Ch. Binek, A. Hochstrat, and W. Kleemann, Phys. Status Solidi A **189**, 575 (2002).